

# AAV-mediated Tyrosinase Gene Transfer Restores Melanogenesis and Retinal Function in a Model of Oculo-cutaneous Albinism Type I (OCA1)

Annagiusti Gargiulo<sup>1</sup>, Ciro Bonetti<sup>1</sup>, Sandro Montefusco<sup>1</sup>, Simona Neglia<sup>1</sup>, Umberto Di Vicino<sup>1</sup>, Elena Marrocco<sup>1</sup>, Michele Della Corte<sup>2</sup>, Luciano Domenici<sup>3,4</sup>, Alberto Auricchio<sup>1</sup> and Enrico M Surace<sup>1</sup>

<sup>1</sup>TIGEM, Telethon Institute of Genetics and Medicine, Napoli, Italy; <sup>2</sup>Department of Ophthalmology, Second University of Napoli, Napoli, Italy; <sup>3</sup>Department "Scienze e Tecnologie Biomediche," School of Medicine, University of L'Aquila, L'Aquila, Italy; <sup>4</sup>Institute of Neuroscience (CNR), Pisa, Italy

Oculo-cutaneous albinism type 1 (OCA1) is characterized by congenital hypopigmentation and is due to mutations in the *TYROSINASE* gene (*TYR*). In this study, we have characterized the morpho-functional consequences of the lack of tyrosinase activity in the spontaneous null mouse model of OCA1 (*Tyr<sup>c-2j</sup>*). Here, we show that adult *Tyr<sup>c-2j</sup>* mice have several retinal functional anomalies associated with photoreceptor loss. To test whether these anomalies are reversible upon *TYR* complementation, we performed intraocular administration of an adeno-associated virus (AAV)-based vector, encoding the human *TYR* gene, in adult *Tyr<sup>c-2j</sup>* mice. This resulted in melanosome biogenesis and *ex novo* synthesis of melanin in both neuroectodermally derived retinal pigment epithelium (RPE) and in neural crest-derived choroid and iris melanocytes. Ocular melanin accumulation prevented progressive photoreceptor degeneration and resulted in restoration of retinal function. Our results reveal novel properties of pigment cells and show that the developmental anomalies of albino mice are associated with defects occurring in postnatal life, adding novel insights on OCA1 disease pathogenesis. In addition, we provide proof-of-principle of an effective gene-based strategy relevant for future application in albino patients.

Received 23 December 2008; accepted 20 April 2009; published online 12 May 2009. doi:10.1038/mt.2009.112

## INTRODUCTION

Melanin protects the skin and eyes against the harmful consequences of environmental light radiation.<sup>1</sup> Pigmented cells, deriving from the neural crest or neuroectoderm, synthesize melanin within specialized organelles: the melanosomes.<sup>2</sup> Neural crest-derived melanocytes reside in the skin and in extra-retinal tissues of the eye, including the choroid and the iris stroma, whereas the retinal pigment epithelium (RPE) is a neuroectoderm-derived highly differentiated monolayer of pigmented cells overlying photoreceptor outer segments, and is critical for proper retinal function.<sup>3,4</sup> Melanosome biogenesis and melanin deposition in both choroidal

and iris melanocytes and in RPE cells of the retina occur mainly during fetal development and early postnatal life.<sup>5</sup> Whether melanosome biogenesis and melanin turnover actively occur in ocular pigment cells during adulthood is still controversial.<sup>6,7</sup>

The biological role of melanin has been extensively studied and partially unraveled through the use of genetically manipulated or spontaneous mutant animals. Among various genetic models of pigment deficiency, oculo-cutaneous albinism type 1 (OCA1, MIM 203100), due to mutations in the *TYROSINASE* (*TYR*) gene, represents the archetype.<sup>8,9</sup> Tyrosinase is a membrane-bound copper enzyme that catalyzes the first two rate-limiting steps of melanin biosynthesis occurring during stages III and IV of melanosome maturation.<sup>10</sup> During stages I and II of melanosome biogenesis, intraluminal fibril is deposited in immature melanosome vesicles.<sup>11</sup> Melanin synthesis begins when tyrosinase is delivered through the early endosome to the melanosome sorting pathway to stage III melanosomes. Melanin synthesis terminates with the complete blackening of stage IV melanosomes.<sup>11,12</sup> Inactivation of the *Tyrosinase* gene leads to a block of melanosome biogenesis in stage II and to a complete lack of pigmentation in melanocytes and RPE cells.<sup>11</sup> The most remarkable consequence of melanin deficiency affects the eye and the visual system. During development, in OCA1 and similarly in other forms of albinism, the lack of melanin within melanosomes critically impacts the fate of ganglion retinal cell axons pathfinding, eventually leading to abnormal segregation of the ipsilateral component of the optic nerve projections to the respective brain targets.<sup>13</sup> Both in humans and nonhuman primates, melanin deficiency also affects fovea development and is associated with uncontrolled pendular eye movements, nistagmus.<sup>8</sup> Besides the role of pigmentation during ocular development, melanin also acts as a filter, by modulating the proper scattering of incoming photons to the eye, and protecting the retina from light-damage.<sup>14,15</sup> In addition, in postnatal life melanin appears to play a key role in photoreceptor physiology, although its effective function is at least in part contradictory.<sup>16-20</sup>

Gene-based strategies have been employed to correct different forms of inherited retinal diseases in animal models.<sup>21</sup> Among vector-based delivery vehicles, those derived from DNA single-stranded adeno-associated virus (AAV) are very promising

Correspondence: Enrico M Surace, Telethon Institute of Genetics and Medicine, Via Pietro Castellino, 111, 80131 Napoli, Italy. Fax +11 39 081 6132351. E-mail: surace@tigem.it

for gene therapy protocols.<sup>22</sup> The availability of dozens of AAV serotype variants converted in recombinant vectors allows to tailor the delivery of therapeutic genetic material in different tissues with high transduction efficiency and specificity.<sup>23–25</sup> AAV2/2, 2/1, and 2/4 have been successfully used to revert the phenotype of different retinal disease models affecting primarily RPE.<sup>26</sup> The evidence of efficacy and safety demonstrated by AAV used in the dog model of Leber's congenital amaurosis, due to deficiency of the *RPE65* gene, has paved the way to three independent human clinical studies.<sup>27–29</sup>

The purpose of this study was (i) to define the phenotypic characteristics of the albino *Tyrosinase*-deficient retina in detail (ii) to investigate whether postnatal AAV-mediated gene transfer of the *TYR* gene to the adult albino retina restores melanosome biogenesis and corrects pigment ocular defects, and (iii) to assess whether this in turn impacts retinal function.

## RESULTS

### Visual function impairment in the albino *Tyrc<sup>-2j</sup>* retina

Previous studies reported functional retinal anomalies in albino mice lacking melanin pigment. To reproduce these findings with

our electrophysiological setting and to generate baseline measurements as reference for assessing gene transfer efficacy, we recorded electrophysiological parameters in C57BL/6J-c2J (*Tyrc<sup>-2j</sup>*) mice compared to genetically identical (coisogenic) C57BL/6J ones. We first measured Ganzfeld flash dark-adapted scotopic and photopic electroretinogram (ERG) responses in 1- to 3-month-old animals, reared in normal light conditions (12-hour light/12-hour dark cycle, maximum light intensity <100 lux). In contrast to previous studies suggesting either strong reduction of photoreceptor responses<sup>30</sup> or absence of any anomaly across pigmented and albino mice,<sup>19</sup> we found a modest but significant reduction of *a*- and *b*-wave amplitudes at high luminance in extensive recording of rods-derived scotopic ERG 1- to 3-month-old animals compared to pigmented animals ( $P = 0.0003$ ; **Figure 1a,b**). To assess whether these abnormalities are progressive in nature, we analyzed the same group of animals 6 months later (7–9 months old). *Tyrc<sup>-2j</sup>* albino ERG responses were further decreased with scotopic *a*- and *b*-maximum amplitudes of  $215 \pm 13 \mu\text{V}$  (mean  $\pm$  SEM) and  $480 \pm 27 \mu\text{V}$ , respectively, compared to a maximum *a*-wave of  $294 \pm 10 \mu\text{V}$  and *b*-wave of  $765 \pm 28 \mu\text{V}$  in pigmented age-matched controls ( $P = 0.00002$ ; **Figure 1a,b**). Cone-derived photopic

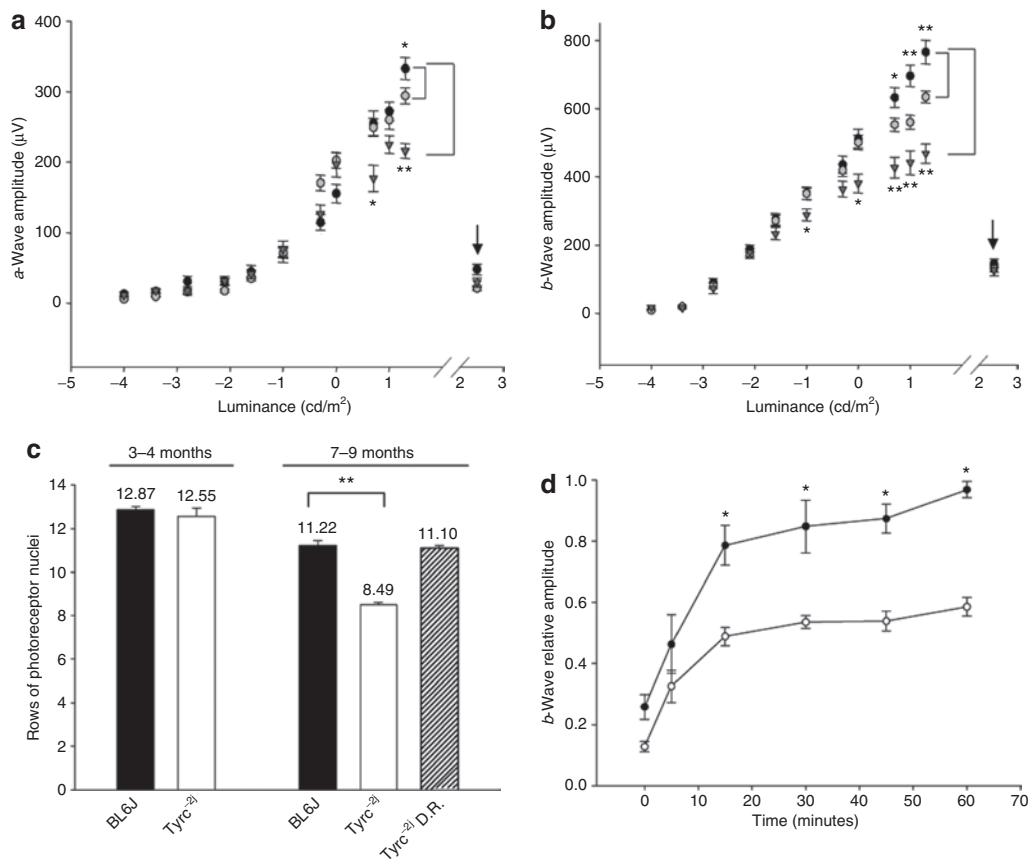


**Figure 1** Characterization of *Tyrc<sup>-2j</sup>* mouse retinal function. **(a)** *a*- and **(b)** *b*-wave amplitudes under scotopic and photopic conditions in C57BL/6J pigmented and in C57BL/6J-c2J (*Tyrc<sup>-2j</sup>*) albino mice. The amplitudes (mean  $\pm$  SEM) evoked by increasing light intensities under scotopic conditions in 1- to 3-month-old (gray circles,  $n = 43$  eyes) and 7- to 9-month-old (filled triangles,  $n = 14$  eyes) *Tyrc<sup>-2j</sup>* mice, as well as 7- to 9-month-old controls (black circles,  $n = 30$  eyes) are shown. Photopic conditions are indicated by an arrow. **(c)** Rows of photoreceptor nuclei in normal C57BL/6J and *Tyrc<sup>-2j</sup>* mice (black and white bars, respectively) at both 1–3 months ( $n = 4$  eyes) and 7–9 months (pigmented  $n = 4$ ; albino  $n = 7$  eyes) of age. *Tyrc<sup>-2j</sup>* mice dark-reared (D.R.) since birth and analyzed at 9 months are represented in striped columns ( $n = 5$  eyes). **(d)** Recovery of *b*-wave amplitude, relative to prebleach baseline levels (1  $\text{cd}/\text{m}^2/\text{s}$ ), after bleaching (300  $\text{cd}/\text{m}^2$  for 3 minutes) in 1-month-old *Tyrc<sup>-2j</sup>* (empty squares,  $n = 20$  eyes) and wild-type age-match C57BL/6J mice (black circles,  $n = 6$  eyes). Asterisks depict statistical significance (*t*-test,  $*P < 0.01$ ;  $**P < 0.0003$ ).

responses were unaffected at both time points. Histological analysis of 1- to 3-month-old *Tyr<sup>c-2j</sup>* mice retinas did not show any apparent photoreceptor loss, whereas a significant reduction of rows of photoreceptor nuclei was observed in 7- to 9-month-old *Tyr<sup>c-2j</sup>* mice (~8 rows of photoreceptor nuclei) compared to pigmented controls (~11 rows of photoreceptor nuclei), indicating that worsening of photoreceptor function is due, at least in part, to a progressive retinal degeneration (Figure 1c). To determine whether these photoreceptor morpho-functional impairments are due to environmental light-induced damage, we reared *Tyr<sup>c-2j</sup>* and wild-type animals in the dark from birth. ERG analysis revealed similar responses in dark-reared *Tyr<sup>c-2j</sup>* and wild-type animals (data not shown); in addition, retinal histological analysis at 7–9 months demonstrated a complete prevention of photoreceptor loss in light-protected *Tyr<sup>c-2j</sup>* animals (Figure 1c). As it has been shown that ERG procedures may result in retinal damage,<sup>31</sup> we measured the ERG responses in an independent group of animals directly at 9 months. The photo-responses were equally lowered as those that were recorded at both early and late stages (data not shown).

Previous studies have showed that several albino rodents display delayed recovery of photoreceptor responses when first challenged with a bright-light stimulus.<sup>17,19</sup> Thus, we measured the kinetics of recovery in *b*-wave amplitude elicited by a test flash (1 cd s/m<sup>2</sup>), following exposure to an intense bright light (conditioning flash; 300 cd/m<sup>2</sup> for 3 minutes), in two cohorts of young (1 month old) *Tyr<sup>c-2j</sup>* animals reared either in normal light (before the onset of retinal degeneration) or in the dark. At 30 minutes rod *b*-wave, the recovery from the conditioning light was 48% in albino and 80% in pigmented animals of the preconditioning amplitude (Figure 1d). A similar delay of recovery was observed in dark-reared albino animals (data not shown). In addition, measurements of the minimal light intensity able to trigger a retinal photo-response (retinal light sensitivity) showed that the lowest light stimulus necessary to generate a *b*-wave response was ~0.5 log unit higher in albino animals with respect to pigmented controls (*Tyr<sup>c-2j</sup>* mean ± SEM = 0.00114 ± 0.00018 cd s/m<sup>2</sup>, *n* = 13; pigmented controls = 0.00402 ± 0.0008 cd s/m<sup>2</sup>, *n* = 11; *P* ≤ 0.001).

Collectively, these results indicate that the *Tyr<sup>c-2j</sup>* albino mouse develops progressive photoreceptor degeneration due to environmental light. In addition, these data support the hypothesis that, independent of light history (light-damage), the kinetics of recovery of photoreceptor function after photobleach is severely impaired in *Tyrosinase*-deficient mice. In addition, despite the absence of melanin, light sensitivity in *Tyr<sup>c-2j</sup>* albino mice is lower compared to pigmented controls.

### Melanosome biogenesis and *ex novo* biosynthesis of melanin following ocular AAV administration to *Tyr<sup>c-2j</sup>* mice

In order to explore whether the pigmentation defects and the electrophysiological anomalies of *Tyrosinase*-deficient albino mice are reversible, we generated an AAV2/1 vector harboring the human *TYR* gene (whose homology with respect to the murine *tyrosinase* coding sequence corresponds to 84%) under the transcriptional control of the ubiquitous cytomegalovirus (CMV) promoter. We performed subretinal injections of 1 × 10<sup>9</sup> genome copies of AAV2/1-CMV-*hTYR* in 1-month-old *Tyr<sup>c-2j</sup>* albino mice, whereas

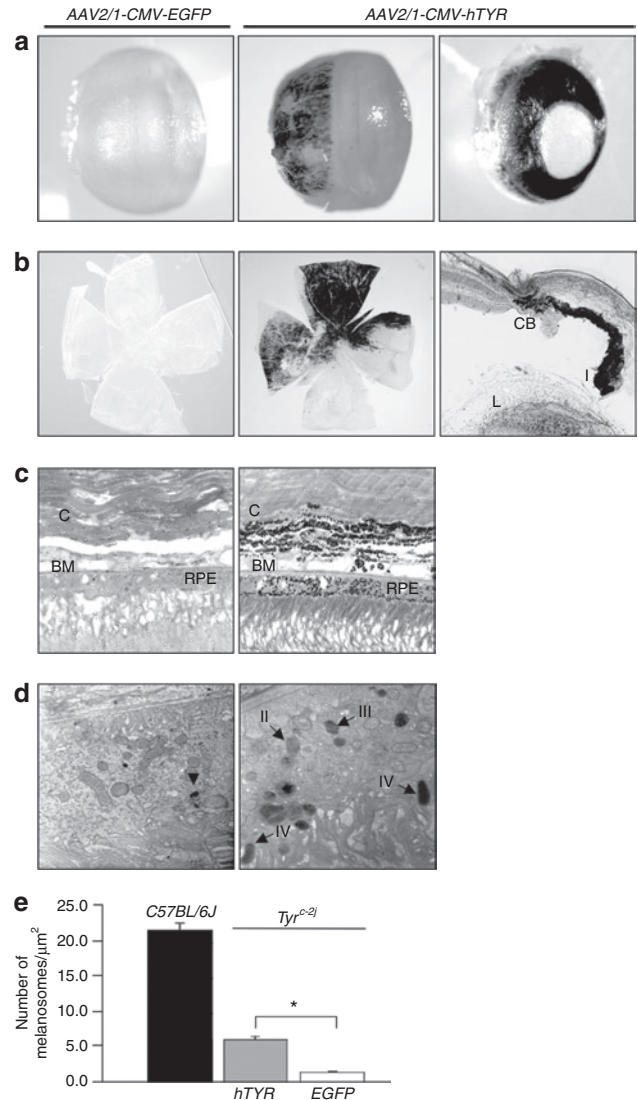


**Figure 2** AAV2/1-mediated ocular gene transfer restores pigmentation in *Tyr<sup>c-2j</sup>* mice. **(a)** External appearance of *Tyr<sup>c-2j</sup>* mice eyes treated subretinally or in the posterior chamber at P30 and analyzed at 1 month of age. Left and middle panels show subretinal-injected eyes treated with AAV2/1-CMV-EGFP (left panel) and AAV2/1-CMV-*hTYR* (middle panel) vectors, respectively. The right panel shows *Tyr<sup>c-2j</sup>* mice eyes injected with AAV2/1-CMV-*hTYR* in the posterior chamber. **(b)** Flat-mounted retinas of 8-month-old *Tyr<sup>c-2j</sup>* mice treated subretinally at P30 with the control (left panel) and the therapeutic vectors (middle panel), respectively. The right panel shows the histological section of the iris of 8-month-old *Tyr<sup>c-2j</sup>* mice injected at 1 month with AAV2/1-CMV-*hTYR* injected in the posterior chamber. I, iris; CB, ciliary body; L, lens. Magnification ×20. **(c)** Semi-thin sections of 2-month-old *Tyr<sup>c-2j</sup>* treated and control mice retinas injected at P30 with AAV2/1-CMV-*hTYR* and AAV2/1-CMV-EGFP, respectively. C, choroids; BM, Bruch's membrane; RPE, retinal pigment epithelium. Magnification ×100. **(d)** Electron microscopy analysis of the RPE from 2-month-old *Tyr<sup>c-2j</sup>* mice injected subretinally at 1 month of age with AAV2/1-CMV-EGFP (left) and the contralateral eye with AAV2/1-CMV-*hTYR* (right). Black arrows indicate melanosomes at different stages of maturation (from stage I to IV) in the eye treated with AAV2/1-CMV-*hTYR* vector (right). The black arrowhead in the control retina (left) depicts a lipofuscin deposit. Magnification ×6,000. **(e)** Number of melanosomes at different stages of maturation in the RPE of C57BL/6J (black bar) and *Tyr<sup>c-2j</sup>* mice injected subretinally with AAV2/1-CMV-*hTYR* or AAV2/1-CMV-EGFP (gray and white bars, respectively; *n* = 3 eyes/group). Asterisks depict statistical significance (*t*-test, *P* < 0.05).

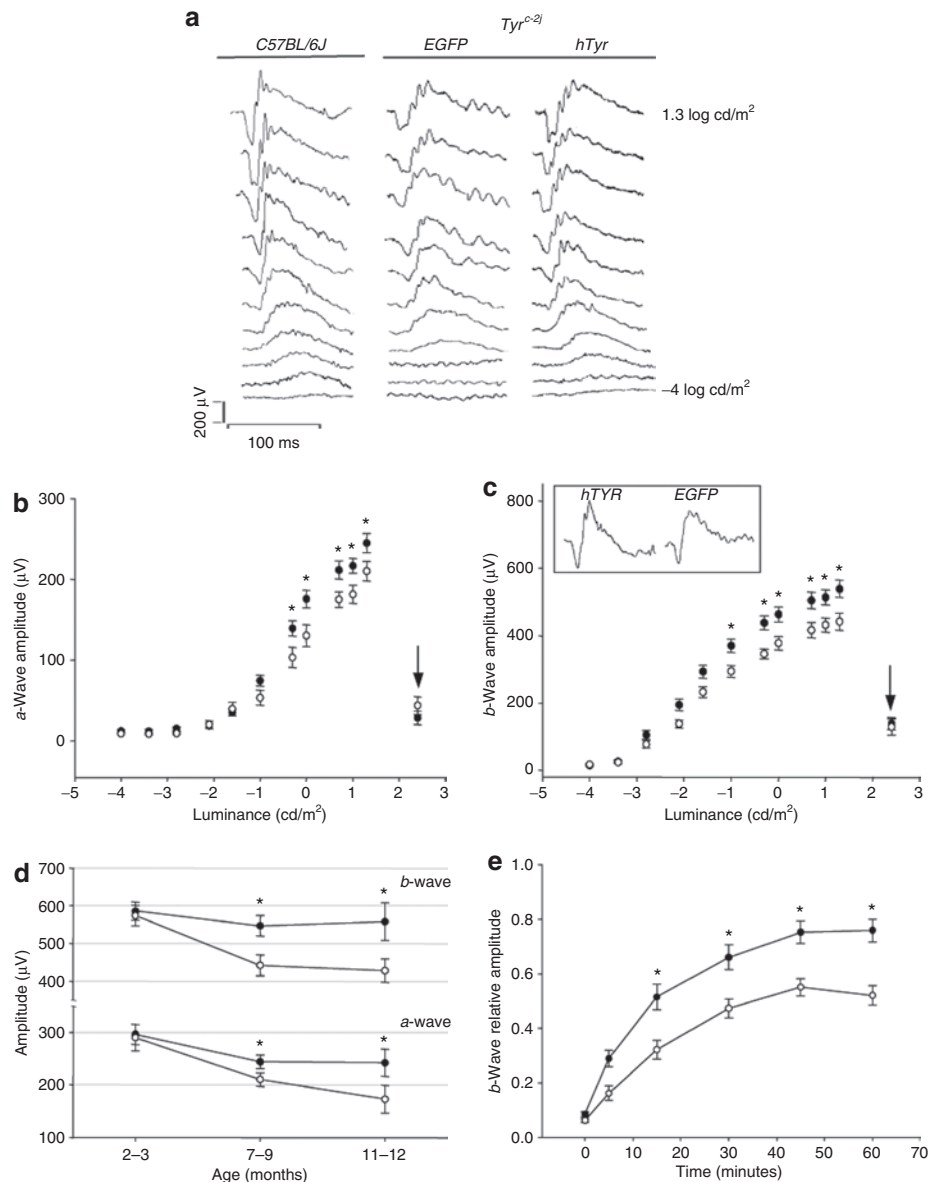


**Figure 3** Retinal functional recovery following AAV2/1-CMV-*hTYR* treatment in *Tyr<sup>c-2j</sup>* mice. **(a)** Representative serial dark-adapted ERG recordings to increasing intensities of light stimuli in 2-month-old C57BL/6J pigmented animal (left) and *Tyr<sup>c-2j</sup>* mice treated with AAV2/1-CMV-EGFP (middle) or AAV2/1-CMV-*hTYR* (right) at one month of age. AAV2/1-CMV-*hTYR* treatment elicits lower light intensities *b*-waves responses compared to AAV2/1-CMV-EGFP injected controls. The traces shown are the average of three responses for each light stimulus. **(b)** *a*- and **(c)** *b*-wave amplitudes (mean ± SEM) under scotopic and photopic (arrows) conditions recorded 6–8 months (7- to 9-month-old animals) after subretinal administration of AAV2/1 vectors harboring *hTYR* (black circles, *n* = 22) or EGFP (empty circles, *n* = 21) genes in *Tyr<sup>c-2j</sup>* mice. In the rectangle in C representative responses generated by 20 cd/m<sup>2</sup>/s light stimulus in a 7-month-old *Tyr<sup>c-2j</sup>* mouse treated with AAV2/1-CMV-*hTYR* (left) and AAV2/1-CMV-EGFP (right) at P30. **(d)** *a*- and *b*-wave maximum amplitudes in *Tyr<sup>c-2j</sup>* mice recorded 1–2, 6–8, and 10–11 months after treatment at P30 with AAV2/1-CMV-*hTYR* (black circles) and AAV2/1-CMV-EGFP (empty circles) vectors. **(e)** Recovery of *b*-wave amplitude in 2- to 3-month-old *Tyr<sup>c-2j</sup>* mice injected subretinally with AAV2/1-CMV-*hTYR* (black circles, *n* = 16) or AAV2/1-CMV-EGFP (empty triangles, *n* = 16) at P30. Asterisks depict statistical significance (*t*-test, *P* < 0.05).

the fellow eye received the same vector dose of an AAV2/1-CMV-EGFP (expressing the enhanced green fluorescence protein) as control. Four weeks after delivery, pigmentation was evident in the enucleated eyes in the portion of the retina exposed to the vector (Figure 2a). In addition, in three animals injected in the posterior chamber of the eye (see Materials and Methods) we observed an intense and diffuse pigmentation of the entire iris (Figure 2a,b, right panels). Histological analysis of subretinal

treated eyes demonstrated the presence of melanin pigment in the RPE and in the choroid, which was likely due to vector leakage (Figure 2a–c, middle panels). Ultrastructural analysis (electron microscopy) of RPE in the treated retinas showed the presence of pigmented stage III and fully mature stage IV melanosomes, while in the untreated portion and in the contralateral retinas, melanosomes were blocked at stage II and completely depleted of pigment (Figure 2d). Despite the use of a ubiquitous promoter,

we did not observe melanin deposits in physiologically nonpigmented cells, such as photoreceptors, as expected for the absence of the melanin biosynthetic pathway in nonpigmented cells. To determine whether the expression of Tyrosinase restores defects in melanosome biogenesis, we counted the total number of melanosomes in RPE of treated and control *Tyr<sup>c-2j</sup>* mice. We observed a significant increase in number of melanosomes per RPE cell per section in treated *Tyr<sup>c-2j</sup>* mice (mean  $\pm$  SEM =  $6.3 \pm 2.3$  melanosomes;  $n = 3$ ) compared to *EGFP* controls ( $1.3 \pm 0.5$  melanosomes  $n = 3$ ; **Figure 2e**), indicating an activation of melanosome biogenesis in treated mice. AAV2/1-CMV-*hTYR*-mediated delivery at birth (postnatal day 0; P0) and in adult *Tyr<sup>c-2j</sup>* retina (P180) also resulted in *ex novo* melanin biosynthesis in RPE and in the choroid (data not shown), suggesting that deposition of melanin and consecutive pigmentation of the eye are reversible when treated, regardless of the age of the animals.

### Long-term retinal functional amelioration after AAV-mediated Tyrosinase gene delivery

ERG analysis of 2- to 3-month-old *Tyr<sup>c-2j</sup>* mice that received subretinal injection of AAV2/1-CMV-*hTYR* at 1 month of age showed no difference compared to control AAV2/1-CMV-*EGFP* injected animals (**Figure 3a**). In contrast, eyes treated with the therapeutic vector responded at  $\sim 0.4$  log unit lower stimuli than *EGFP* injected controls eyes 1 month after treatment, indicating an improvement of retinal light sensitivity (**Figure 3a**; *Tyr<sup>c-2j</sup>* TYR-treated mean  $\pm$  SEM =  $0.0018 \pm 0.00032$  cd/s/m<sup>2</sup>,  $n = 20$ ; *Tyr<sup>c-2j</sup>* *EGFP* control =  $0.0067 \pm 0.0011$  cd/s/m<sup>2</sup>,  $n = 20$ ;  $P \leq 0.0001$ ). ERG responses recorded in 7- to 9-month-old animals (6–8 months after vector delivery) showed a significant prevention of both *a*- and *b*-wave amplitudes reduction (at the maximal amplitude,  $P = 0.04$  and  $P = 0.004$ , respectively), otherwise present in the contralateral control eye (**Figure 3b,c**; *a*- and *b*-wave amplitude *Tyr<sup>c-2j</sup>* TYR-treated mean  $\pm$  SEM =  $244 \pm 13$  and  $547 \pm 27$ , respectively; *Tyr<sup>c-2j</sup>* *EGFP* control =  $210 \pm 14$  and  $442 \pm 28$ , respectively). Similarly, ERG analysis performed in the same animals at 11–12 months of age showed *a*- and *b*-wave amplitudes comparable to 3- to 4-month-old treated retinas, indicating that protection is maintained on the long-term (**Figure 3d**). ERG analysis was performed to determine the ability to recover from photoreceptor desensitization in the same cohorts of animals (2–3 months old). As shown in **Figure 3e**, an amelioration of the kinetics of *b*-wave recovery after bright-light exposure was observed in *Tyr<sup>c-2j</sup>* retinas treated with the therapeutic vector compared to controls. In order to determine whether over-expression of *TYR* hesitates in alterations of ERG responses and in detrimental effects on retinal function, we injected 1-month-old C57/BL6 mice subretinally with AAV2/1-CMV-*TYR* in one eye, whereas the fellow eye received AAV2/1-CMV-*EGFP* or was left untreated. Both thresholds and *a*- and *b*-scotopic and photopic retinal ERG responses remained unchanged among the three groups, thus suggesting that *TYR* over-expression does not influence photoreceptor function in normally pigmented eyes (data not shown).

These data indicate that restored tyrosinase activity and ocular melanin accumulation result in stable protection of photoreceptor function from environmental light-damage and in significant improvement of both retinal sensitivity and ability to recover from desensitization.

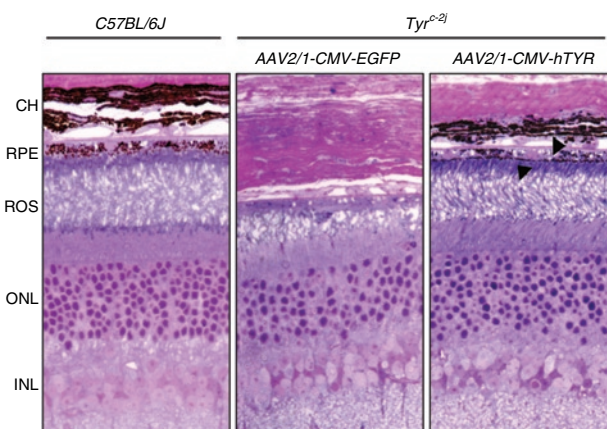


**Figure 4** Morphological analysis of *Tyr<sup>c-2j</sup>* retinas following AAV-mediated gene transfer. Semi-thin sections of 8 months old C57BL/6J (left) and *Tyr<sup>c-2j</sup>* mice treated at P30 with AAV2/1-CMV-*EGFP* (middle) and AAV2/1-CMV-*hTYR* (right). Arrowheads indicate the presence of melanin in the RPE and in choroid cells. CH, choroid; INL, inner nuclear layer; ONL, outer nuclear layer; ROS, rods outer segment; RPE, retinal pigment epithelium.

### Preservation of photoreceptors from light damage following gene transfer

To determine whether the functional recovery is associated with prevention of photoreceptor loss from environmental light-damage, we histologically quantified the rows of photoreceptor nuclei in 7- to 9-month-old *Tyr<sup>c-2j</sup>* animals that received AAV therapeutic and control vectors at 1 month of age. We observed significant differences between AAV2/1-CMV-*hTYR*-treated retinas compared to AAV2/1-CMV-*EGFP* controls (*Tyr<sup>c-2j</sup>* TYR treated mean  $\pm$  SEM =  $10.79 \pm 0.14$ ; *Tyr<sup>c-2j</sup>* *EGFP* treated =  $8.14 \pm 0.14$ ;  $P \leq 0.01$ ,  $n = 5$  and  $4$ , respectively). **Figure 4** shows the outer nuclear layer of 9-month-old *Tyr<sup>c-2j</sup>* retinas treated at P30. Of note, the fact that the number of photoreceptor nuclei was preserved throughout the retina, irrespective of the transduced (pigmented) and nontransduced portions of the treated eyes. These histological findings are consistent with electrophysiological results.

## DISCUSSION

In this study we dissected five distinct morpho-functional aspects of tyrosinase deficiency in ocular-pigmented cells: (i) lack of melanin, (ii) reduction of the number of melanosomes, (iii) progressive decrease of photoreceptor responses due to environmental light-induced degeneration, (iv) low retinal sensitivity to dim light, and (v) delayed recovery from photoreceptor desensitization. These characteristic features of albinism were all significantly restored by AAV-mediated *TYR* gene complementation.

The expression of *Tyrosinase* and other genes, such as *P* and *GPR143* (*Oa1*) genes, involved in pigmentation and associated with different forms of albinism correlates with retinal development and with the segregation of ganglion cell axons at the optic chiasm in the brain.<sup>32,33</sup> *Tyrosinase* expression in the mouse retina begins at embryonic day 10.5 (E10.5) during early retinal differentiation and peaks at E14 in the RPE and between P1 and P8 in the choroidal melanocytes.<sup>5,32</sup> It has been reported that in the adult eye *Tyrosinase* expression and activity is barely detectable in the RPE, whereas in

the choroid it progressively declines after the first postnatal week and is then largely lost in the adult retina.<sup>5,6</sup> We demonstrated that AAV-mediated expression of the *Tyrosinase* gene leads to melanosome biogenesis and melanin synthesis at any age of delivery (P0, P30, P180). Indeed, we showed that the *Tyr<sup>c-2j</sup>* retinas transduced with AAV2/1-encoding *TYR* harbor melanosomes at different stages of maturation including fully pigmented stage IV melanosomes. This finding implies that the sorting pathways to deliver the tyrosinase enzyme from the early endosomes to stage II melanosomes are active in adult RPE and ocular melanocytes, and that proteins involved in the melanin synthetic pathway are capable of producing melanin upon tyrosinase expression. This result conclusively demonstrates that both adult neuroectodermal-derived RPE and neural crest-derived ocular-pigmented cells are fully competent to actively synthesize melanin in postnatal life. The ability of the RPE to activate melanosome biogenesis and protein turnover in postnatal life is further supported by AAV vector-mediated *Oa1* gene transfer to the adult retina of the *Oa1<sup>-/-</sup>* mice.<sup>34</sup> Whereas *Oa1* controls melanosome biogenesis at early stages and *Oa1* gene complementation increases the number of melanosomes by triggering stage I endolysosome–premelanosome formation,<sup>34,35</sup> in this study the higher number of melanosomes in *TYR*-treated retinas appears to be due to melanin deposition in stage II melanosomes, thereby suggesting that melanin biosynthesis exerts a positive feedback on melanosome organogenesis. It has been recently suggested that L-DOPA, an intermediate of tyrosinase-mediated melanin biosynthesis, is the ligand of *Oa1* protein,<sup>36</sup> thereby indicating that tyrosinase activity is coupled to *Oa1* signaling through L-DOPA synthesis. Thus, our results support a model in which tyrosinase expression generates L-DOPA, eventually leading to *Oa1*-mediated melanosome biogenesis.

Excessive light exposure can result in experimental retinal degeneration in albino mice.<sup>14,15</sup> Typically, experimental light-damage is conducted in albino rodents because they lack melanin in the choroid, iris and RPE, thus increasing the amount of light reaching the retina, eventually leading to an excessive phototransduction signaling. Genetic studies indicate that key molecular players, triggering light-induced photoreceptor cell apoptosis, are associated with rhodopsin activation, rhodopsin shutoff, and visual cycle rate.<sup>15</sup> In this study, we showed that *Tyr<sup>c-2j</sup>* mice are susceptible to normal environmental light, despite the presence of the Leu450 variation in the *RPE65* gene, that was shown to give a relative resistance to experimental light-damage compared to *BALB/c* albino mice.<sup>19,37,38</sup> As further support to this finding, we showed that both dark rearing and melanin synthesis after *Tyrosinase* gene complementation by AAV retinal gene transfer protect the albino retina from light-induced photoreceptor loss. Interestingly, we observed prevention of photoreceptor degeneration throughout the retina; nevertheless, pigmentation was restricted to the portion of the retina exposed to the AAV vector (corresponding to 1/2–1/3 of the total retina surface; **Figure 2**), thus suggesting that the absorption of light by the transduced pigmented area reduces excessive retinal light scattering, thereby exerting a beneficial effect to the entire retina.

The slowed recovery of photoreceptor function following bright-light exposure in albino mice and its improvement in AAV-treated animals is particularly worth of note, and suggests two hypotheses: (i) the lack of the light-absorbing action of melanin

leads to an increased retinal light exposure that in turn generates a stronger bleach in the albino compared to the pigmented retina, thus lowering the kinetics of recovery in the unpigmented retina; (ii) alternatively, or additionally, the role of melanin within RPE is not exclusively attributable to a mere physical filter to light, but it also exerts a biochemical role on photoreceptor function. This is sustained by two observations. First, we measured a lower retinal light sensitivity in *Tyr<sup>c-2j</sup>* compared to pigmented mice, while in AAV-treated *Tyr<sup>c-2j</sup>* eyes pigmentation is associated with higher light sensitivity. Thus, despite the absence of melanin pigment, the albino retina requires a brighter light intensity to trigger a photo-response than pigmented controls. Second, rod scotopic responses in young *Tyr<sup>c-2j</sup>* mice (before the onset of degeneration) show minimal differences (slight lowering scotopic responses) compared to pigmented animals, even though the effective illuminance is higher in albino than pigmented eyes, due to the lack of melanin filter. These findings are consistent with previous studies,<sup>16,39–42</sup> which suggest that the lower sensitivity of the albino retina is due to the calcium buffering properties of melanin and the consequent higher concentration of calcium in the subretinal space of albino animals.<sup>42</sup> In agreement with our results, a previous study<sup>19</sup> showed a slow recovery from photobleach in *Tyr<sup>c-2j</sup>* mice compared to pigmented controls. However, in contrast with our findings, retinal light sensitivity was found significantly higher in albino mice compared with pigmented mice.<sup>19</sup> Both phenomena (recovery from photobleach and retinal sensitivity) in the previous study were related to “the physical hypothesis” on the role of melanin, *i.e.*, the higher effective ocular illuminance to equal light stimuli in albino mice leads to a higher retinal sensitivity and a delayed recovery from photobleach caused by stronger rhodopsin bleach due to the absence of melanin.<sup>19</sup> A similar argument is generally sustained to explain supernormal ERG responses occasionally found in albino patients.<sup>43,44</sup> These controversies over the impact of tyrosinase activity on retinal function need further studies aimed at precisely dissecting the distinctive “biochemical” and “physical” role of melanin. This will also be crucial from a therapeutic perspective to determine whether the simple external protection from light is beneficial or, as suggested by the retinal sensitivity results in this study, pigmentation is necessary for proper photoreceptor function.

In summary, the results of this study show that AAV-mediated retinal gene delivery of the human *Tyrosinase* gene is able to activate melanosome biogenesis and their melanization. The presence of melanin protects the retina from environmental light-induced degeneration and normalizes photoreceptor activity, such as retinal sensitivity and the ability to recover from photobleach. These data shed light on the role of tyrosinase activity and melanin on photoreceptor function establishing that the disease pathogenesis of oculo-cutaneous albinism is not only characterized by developmental anomalies affecting the visual system, but also recognizes reversible postnatal defects occurring in fully developed eyes. Whereas gene therapy intervention would require *in utero* vector administration to revert the developmental defects present in albinism, such as fovea hypoplasia and misrouting of the optic fibers, in this study, we show that *TYR* treatment ensures correction of these novel postnatal defects. To determine the effective therapeutic impact of this treatment further studies will be necessary to

investigate whether light-induced degeneration, retinal sensitivity, and the ability to recover from photobleach are present in albino patients and to understand their influence on quality of vision. The encouraging safety and efficacy results of three clinical studies aimed at treating an RPE specific genetic defect with the use of AAV<sup>27–29</sup> may support the use of this strategy for a debilitating condition, such as albinism.

## MATERIALS AND METHODS

**Mice.** This study was carried out in accordance with the Association for Research in Vision and Ophthalmology Statement for the Use of Animals in Ophthalmic and Vision Research. Mice were bred and maintained under normal animal house conditions: 12-hour light–dark cycle (maximum light intensity <100lux). Albino C57BL/6J-c2J (*Tyr<sup>c-2j</sup>*) mice,<sup>45</sup> and pigmented C57BL/6J were purchased from the Jackson Laboratory (Bar Harbor, ME) and maintained inbred in the animal house.

**Dark rearing and light susceptibility.** Dark-reared *Tyr<sup>c-2j</sup>* mice ( $n = 7$ ) were kept in ventilated, light-tight cages from postnatal day 2 to 7 months. In order to confirm the presence of the Leu450Met variant affecting the *RPE65* gene in *Tyr<sup>c-2j</sup>* mice genome, associated to light-induced damage susceptibility,<sup>38</sup> DNA derived from mouse tails by standard procedures was PCR-amplified as described.<sup>46</sup>

**Generation of the pAAV2.1-CMV-humanTYR construct, AAV vector production, and purification.** Functional Human *Tyrosinase* coding sequence was obtained by PCR amplification on human RPE immortalized cells (ARPE19) cDNA. PCR was performed using the Fast Start High Fidelity PCR System kit (Roche, Milan, Italy) with the following primers: Tyr – *NotI* – Forward: 5'-AAGCGGCCGCGCCATGCTCCTGGCTGTTTTGTAC-3' and Tyr – *HindIII* – Reverse: 5'-AAGCTTCAAGCCCTGTAATCCCAGCATTTTGGGAGGCC-3'. The PCR product was subcloned in TOPO TA cloning kit (Invitrogen, Milano, Italy), direct sequenced and digested to obtain the hTyr cds with *NotI*–*HindIII* protruding ends. The fragment was cloned into pAAV2.1-CMV-EGFP<sup>47</sup> by removing the *EGFP* coding sequence (*NotI*–*HindIII*). AAV vectors were produced by triple transfection, purified by CsCl<sub>2</sub> ultracentrifugation, and titered (in genome copies/milliliter) using a real-time PCR-based assay and a dot blot analysis as previously described.<sup>47</sup> The TIGEM AAV vector core produced AAV vectors.

### Vector administration.

**Subretinal injection:** Newborn (P0) and adult (P30–180) albino *Tyr<sup>c-2j</sup>* mice were used. Mice were anesthetized with an intraperitoneal injection of avertin at 2 ml/100 g body wt (1.25% (wt/vol) and viral vectors were delivered via a trans-scleral transchoroidal approach as described.<sup>48</sup> Albino mice were injected in the right eye with  $1 \times 10^9$  genome copies of AAV2/1-CMV-hTYR (2  $\mu$ l) and the same dose of AAV2-CMV-EGFP in the left eye, as control.

**Posterior chamber injection:** To transduce the iris, 2  $\mu$ l of the AAV2/1-CMV-hTYR vector was injected in the posterior chamber by inserting the needle via a trans-scleral transchoroidal approach, beyond the suspensory ligament of the lens and the ciliary processes.

**Electrophysiological recordings.** ERG recordings were performed as previously described.<sup>34</sup> ERGs were recorded under two conditions. First, scotopic ERG, obtained with increasing intensities of light flash from  $1 \times 10^{-4}$  to 20.0 cd s/m<sup>2</sup> (–4.0 to +1.3 log cd s/m<sup>2</sup>) (to intervals of 0.6 log unit for each step). Second, photopic ERG, obtained with a single flash of 20.0 cd s/m<sup>2</sup> in the presence of a constant background illumination set at 50 cd/m<sup>2</sup>. Retinal sensitivity to light was assessed as the lowest light stimulus able to evoke a *b*-wave-shaped response in triplicate (only reproducible responses were considered). To assess recovery after photobleach, mice (dark adapted) were exposed to a constant light intensity set at 300 cd/m<sup>2</sup> for 3 minutes (bleaching condition). Time course of photoreceptor activity recovery was

examined by monitoring the growth *b*-wave (recorded in response to a light flash of 1 cd s/m<sup>2</sup>) to intervals of 0, 5, 15, 30, 45, and 60 minutes and compared to *b*-waves recorded before the bleaching of equal flash intensity (1 cd s/m<sup>2</sup>). Data were statistically analyzed using the Statistica (Statsoft, Tulsa, OK: two-way analysis of variance using least significance difference test for pair-wise comparisons).

**Histology.** Mice were enucleated after an intracardiac injection of 4% paraformaldehyde in phosphate-buffered saline. Around 150–200 serial sections (12- $\mu$ m thick) were cut along the horizontal meridian for each eye; the sections were progressively distributed on 10 slides so that each slide contained 15–20 sections representative of the whole eye at different levels. The sections were stained with hematoxylin and eosin according to standard procedures. To quantify the number of photoreceptor nuclei in the outer nuclear layer a minimum of three sections/slide, representative of the entire eyecup, were analyzed as previously described.<sup>49</sup> Semi-thin sections, 1- $\mu$ m thick, were transversally cut on a Leica Ultratome RM2235 (Leica Microsystems, Bannockburn, IL), mounted on slides and stained with toluidine blue on a hot plate.

**Electron microscopy.** Electron microscopy was performed as described.<sup>50</sup> Quantitative analysis of melanosomes was made by counting three different optical fields for each eye. Melanosomes at different stages of maturation (I, II, III, and IV) were evaluated in each micrograph with the following criteria: “stage I” melanosomes exhibited few randomly distributed proteinaceous fibrils and vesicles in their lumen. “Stage II” melanosomes were deprived of vesicles with denser packed proteinaceous fibrils frequently organized in parallel arrays. The fibril arrays were still well visible in “stage III” melanosomes but were darker due to addition of loose melanin depositions. Finally, “stage IV” melanosomes were filled with dense melanin frequently masking fibrillar elements.

## ACKNOWLEDGMENTS

We thank Andrea Ballabio, Graciana Diez Roux (TIGEM), Luciana Borrelli, and Claudio Macaluso for a critical reading of the manuscript; Mariacarmela Allocca for help with the surgery, the TIGEM AAV vector Core and the Telethon Electron Microscopy Core. This work was supported by the Telethon grant TIGEM P21, grant R01EY015136-01 from the NEI, and grant D.M.589/7303/04 from the Italian Ministry of Agriculture.

## REFERENCES

- Goding, CR (2007). Melanocytes: the new Black. *Int J Biochem Cell Biol* **39**: 275–279.
- Marks, MS and Seabra, MC (2001). The melanosome: membrane dynamics in black and white. *Nat Rev Mol Cell Biol* **2**: 738–748.
- Lamb, TD and Pugh, EN Jr. (2004). Dark adaptation and the retinoid cycle of vision. *Prog Retin Eye Res* **23**: 307–380.
- Thompson, DA and Gal, A (2003). Vitamin A metabolism in the retinal pigment epithelium: genes, mutations, and diseases. *Prog Retin Eye Res* **22**: 683–703.
- Lopes, VS, Wasmeyer, C, Seabra, MC and Futter, CE (2007). Melanosome maturation defect in Rab38-deficient retinal pigment epithelium results in instability of immature melanosomes during transient melanogenesis. *Mol Biol Cell* **18**: 3914–3927.
- Schraermeyer, U (1993). Does melanin turnover occur in the eyes of adult vertebrates? *Pigment Cell Res* **6**: 193–204.
- Schraermeyer, U, Kopitz, J, Peters, S, Henke-Fahle, S, Blitgen-Heinecke, P, Kokkinou, D et al. (2006). Tyrosinase biosynthesis in adult mammalian retinal pigment epithelial cells. *Exp Eye Res* **83**: 315–321.
- King RA, Hearing V, Creel DJ and Oetting WS (2001). Albinism. In: Scriver, C, Beaudet, A, Sly, W and Valle, D (eds). *The Metabolic & Molecular Bases of Inherited Diseases*, 8th edn., Vol IV. McGraw-Hill: New York, NY, pp 5903–5933.
- Ray, K, Chaki, M and Sengupta, M (2007). Tyrosinase and ocular diseases: some novel thoughts on the molecular basis of oculocutaneous albinism type 1. *Prog Retin Eye Res* **26**: 323–358.
- Lerner, AB, Fitzpatrick, TB, Calkins, E and Zimmerson, WH (1950). Mammalian tyrosinase: the relationship of copper to enzymatic activity. *J Biol Chem* **187**: 793–802.
- Raposo, G and Marks, MS (2007). Melanosomes—dark organelles enlighten endosomal membrane transport. *Nat Rev Mol Cell Biol* **8**: 786–797.
- Futter, CE (2006). The molecular regulation of organelle transport in mammalian retinal pigment epithelial cells. *Pigment Cell Res* **19**: 104–111.
- Jeffery, G (1998). The retinal pigment epithelium as a developmental regulator of the neural retina. *Eye* **12** (Pt 3b): 499–503.
- LaVail, MM, Gorris, GM, Repaci, MA, Thomas, LA and Ginsberg, HM (1987). Genetic regulation of light damage to photoreceptors. *Invest Ophthalmol Vis Sci* **28**: 1043–1048.

15. Wenzel, A, Grimm, C, Samardzija, M and Reme, CE (2005). Molecular mechanisms of light-induced photoreceptor apoptosis and neuroprotection for retinal degeneration. *Prog Retin Eye Res* **24**: 275–306.
16. Balkema, GW (1988). Elevated dark-adapted thresholds in albino rodents. *Invest Ophthalmol Vis Sci* **29**: 544–549.
17. Behn, D, Doke, A, Racine, J, Casanova, C, Chemtob, S and Lachapelle, P (2003). Dark adaptation is faster in pigmented than albino rats. *Doc Ophthalmol* **106**: 153–159.
18. Green, DG, Herreros de Tejada, P and Glover, MJ (1994). Electrophysiological estimates of visual sensitivity in albino and pigmented mice. *Vis Neurosci* **11**: 919–925.
19. Nusinowitz, S, Nguyen, L, Radu, R, Kashani, Z, Farber, D and Danciger, M (2003). Electroretinographic evidence for altered phototransduction gain and slowed recovery from photobleaches in albino mice with a MET450 variant in RPE65. *Exp Eye Res* **77**: 627–638.
20. Page-McCaw, PS, Chung, SC, Muto, A, Roeser, T, Staub, W, Finger-Baier, KC *et al.* (2004). Retinal network adaptation to bright light requires tyrosinase. *Nat Neurosci* **7**: 1329–1336.
21. Bainbridge, JW, Tan, MH and Ali, RR (2006). Gene therapy progress and prospects: the eye. *Gene Ther* **13**: 1191–1197.
22. Samulski, RJ, Srivastava, A, Berns, KI and Muzyczka, N (1983). Rescue of adeno-associated virus from recombinant plasmids: gene correction within the terminal repeats of AAV. *Cell* **33**: 135–143.
23. Allocca, M, Mussolino, C, Garcia-Hoyos, M, Sanges, D, Iodice, C, Pettillo, M *et al.* (2007). Novel adeno-associated virus serotypes efficiently transduce murine photoreceptors. *J Virol* **81**: 11372–11380.
24. Gao, GP, Alvira, MR, Wang, L, Calcedo, R, Johnston, J and Wilson, JM (2002). Novel adeno-associated viruses from rhesus monkeys as vectors for human gene therapy. *Proc Natl Acad Sci USA* **99**: 11854–11859.
25. Surace, EM and Auricchio, A (2008). Versatility of AAV vectors for retinal gene transfer. *Vision Res* **48**: 353–359.
26. Auricchio, A and Rolling, F (2005). Adeno-associated viral vectors for retinal gene transfer and treatment of retinal diseases. *Curr Gene Ther* **5**: 339–348.
27. Bainbridge, JW, Smith, AJ, Barker, SS, Robbie, S, Henderson, R, Balaggan, K *et al.* (2008). Effect of gene therapy on visual function in Leber's congenital amaurosis. *N Engl J Med* **358**: 2231–2239.
28. Hauswirth, W, Aleman, TS, Kaushal, S, Cideciyan, AV, Schwartz, SB, Wang, L *et al.* (2008). Phase I trial of Leber congenital amaurosis due to RPE65 mutations by ocular subretinal injection of adeno-associated virus gene vector: short-term results. *Hum Gene Ther* (epub ahead of print).
29. Maguire, AM, Simonelli, F, Pierce, EA, Pugh, EN Jr, Mingozzi, F, Bennicelli, J *et al.* (2008). Safety and efficacy of gene transfer for Leber's congenital amaurosis. *N Engl J Med* **358**: 2240–2248.
30. Bravo-Nuevo, A, Walsh, N and Stone, J (2004). Photoreceptor degeneration and loss of retinal function in the C57BL/6-C2J mouse. *Invest Ophthalmol Vis Sci* **45**: 2005–2012.
31. Cideciyan, AV, Jacobson, SG, Aleman, TS, Gu, D, Pearce-Kelling, SE, Sumaroka, A *et al.* (2005). *In vivo* dynamics of retinal injury and repair in the rhodopsin mutant dog model of human retinitis pigmentosa. *Proc Natl Acad Sci USA* **102**: 5233–5238.
32. Beermann, F, Schmid, E and Schutz, G (1992). Expression of the mouse tyrosinase gene during embryonic development: recapitulation of the temporal regulation in transgenic mice. *Proc Natl Acad Sci USA* **89**: 2809–2813.
33. Surace, EM, Angeletti, B, Ballabio, A and Marigo, V (2000). Expression pattern of the ocular albinism type 1 (Oa1) gene in the murine retinal pigment epithelium. *Invest Ophthalmol Vis Sci* **41**: 4333–4337.
34. Surace, EM, Domenici, L, Cortese, K, Cotugno, G, Di Vicino, U, Venturi, C *et al.* (2005). Amelioration of both functional and morphological abnormalities in the retina of a mouse model of ocular albinism following AAV-mediated gene transfer. *Mol Ther* **12**: 652–658.
35. Cortese, K, Giordano, F, Surace, EM, Venturi, C, Ballabio, A, Tacchetti, C *et al.* (2005). The ocular albinism type 1 (OA1) gene controls melanosome maturation and size. *Invest Ophthalmol Vis Sci* **46**: 4358–4364.
36. Lopez, VM, Decatur, CL, Stamer, WD, Lynch, RM and McKay, BS (2008). L-DOPA is an endogenous ligand for OA1. *PLoS Biol* **6**: e236.
37. Danciger, M, Matthes, MT, Yasamura, D, Akhmedov, NB, Rickabaugh, T, Gentleman, S *et al.* (2000). A QTL on distal chromosome 3 that influences the severity of light-induced damage to mouse photoreceptors. *Mamm Genome* **11**: 422–427.
38. Wenzel, A, Reme, CE, Williams, TP, Hafezi, F and Grimm, C (2001). The Rpe65 Leu450Met variation increases retinal resistance against light-induced degeneration by slowing rhodopsin regeneration. *J Neurosci* **21**: 53–58.
39. Drager, UC (1985). Calcium binding in pigmented and albino eyes. *Proc Natl Acad Sci USA* **82**: 6716–6720.
40. Drager, UC and Balkema, GW (1987). Does melanin do more than protect from light? *Neurosci Res Suppl* **6**: S75–S86.
41. Hayes, JM and Balkema, GW (1993). Visual thresholds in mice: comparison of retinal light damage and hypopigmentation. *Vis Neurosci* **10**: 931–938.
42. Lavalley, CR, Chalifoux, JR, Moosally, AJ and Balkema, GW (2003). Elevated free calcium levels in the subretinal space elevate the absolute dark-adapted threshold in hypopigmented mice. *J Neurophysiol* **90**: 3654–3662.
43. Krill, AE and Lee, GB (1963). The electroretinogram in albinos and carriers of the ocular albino trait. *Arch Ophthalmol* **69**: 32–38.
44. Summers, CG, Creel, D, Townsend, D and King, RA (1991). Variable expression of vision in sibs with albinism. *Am J Med Genet* **40**: 327–331.
45. Kwon, BS, Haq, AK, Pomerantz, SH and Halaban, R (1987). Isolation and sequence of a cDNA clone for human tyrosinase that maps at the mouse c-albino locus. *Proc Natl Acad Sci USA* **84**: 7473–7477.
46. Kim, SR, Fishkin, N, Kong, J, Nakanishi, K, Allikmets, R and Sparrow, JR (2004). Rpe65 Leu450Met variant is associated with reduced levels of the retinal pigment epithelium lipofuscin fluorophores A2E and iso-A2E. *Proc Natl Acad Sci USA* **101**: 11668–11672.
47. Auricchio, A, Kobinger, G, Anand, V, Hildinger, M, O'Connor, E, Maguire, AM *et al.* (2001). Exchange of surface proteins impacts on viral vector cellular specificity and transduction characteristics: the retina as a model. *Hum Mol Genet* **10**: 3075–3081.
48. Liang, FQ, Anand, V, Maguire, A and Bennett, J (2000). Intraocular delivery of recombinant virus. *Meth Mol Med* **47**: 125–139.
49. Rex, TS, Allocca, M, Domenici, L, Surace, EM, Maguire, AM, Lyubarsky, A *et al.* (2004). Systemic but not intraocular Epo gene transfer protects the retina from light-and genetic-induced degeneration. *Mol Ther* **10**: 855–861.
50. Allocca, M, Doria, M, Pettillo, M, Colella, P, Garcia-Hoyos, M, Gibbs, D *et al.* (2008). Serotype-dependent packaging of large genes in adeno-associated viral vectors results in effective gene delivery in mice. *J Clin Invest* **118**: 1955–1964.